*Pure & Appl. Chem.*, Vol. 64, No. 10, pp. 1421–1435, 1992.
Printed in Great Britain.


# Multiple weak forces in ion-binding molecules

A. Shanzer[a], J. Libman[a] and S. Lifson[b]

Departments of Organic Chemistry[a] and of Chemical Physics[b],
The Weizmann Institute of Science, Rehovot, 76100 Israel.

ABSTRACT

Natural ion binding molecules, specifically iron(III) carriers, are used as guiding models for the preparation of synthetic binders. This biomimetic approach takes advantage of the evolutionary edge of natural molecules and aims at reproducing the essential characteristics of the most potent natural compounds with the simplest possible synthetic structures.

The potent Enterobactin siderophore is examined as a guiding model. Its H-bonding (hydrogen-bonding) network and elements of preorganization are reproduced with all-synthetic, $C_3$-symmetric, chiral Triscatecholates to provide efficient and selective iron(III) binders of high optical purity. The structural principles operating in Enterobactin are then applied to the synthesis of Ferrichrome analogs, but with a shift of emphasis to conformational characteristics and biological activity. Comparison between two homologous families of Trishydroxamates demonstrates the role of H-bonding networks and van-der-Waals interactions in dictating the complexes' isomeric and optical purity, and highlights the conformational consequences of H-bonds. Some analogs of Ferrichrome reproduce the function of the natural compound as microbial iron(III) carriers by binding to both membrane receptors and transport proteins. Other derivatives inhibit the performance of the natural carriers by blocking the membrane receptors. The three strands of the $C_3$-symmetric ligands are extended, each carrying two hydroxamates, to become ditopic ion binders. These ligands form triple-stranded, helical metal complexes which are stabilized by H-bond networks and allow systematic extension to polynuclear complexes.

Our design was governed by a few basic principles. We separated functional elements from structural elements, and used chiral elements as structural probes. To allow systematic modifications we adopted a modular synthetic strategy, and made use of variable modules as building blocks. As a common theme we applied multiple weak forces, particularly H-bond networks, to shape the individual molecules, stabilize their complexes and possibly favor their assembly to supramolecular architectures. Throughout all stages of this work physicochemical and biological testing of the compounds was joined by theoretical calculations in order to put experimental observations into a coherent structural framework.

## 1. INTRODUCTION

No living cell could exist without specific transport of ions across its membrane. Ion-carriers comprise one of the tools nature developed to perform this task. Ion-carriers vary widely in chemical composition and geometry, but they all function by the same three essential elements: high selectivity, high efficiency and high permeability across the cell membrane. Among these carriers, two major families may be discerned: those that transport alkali metal ions, termed ionophores[1-2], and those that transport iron(III), termed siderophores[3-6]. The major difference between the two families of compounds is the mode by which they permeate biological membranes. The former act by diffusion, which is driven by the concentration gradients across the membranes. The latter are taken up through the

intervention of specific receptors and transport proteins in an energy driven process. This process allows intracellular accumulation of iron(III) against unfavorable concentration gradients so as to maintain the intracellular iron(III) level within the required narrow window. Due to their different modes of permeation, the envelopes of ionophores and siderophores differ greatly. While ionophores possess a rather hydrophobic envelope suitable to transverse any hydrophobic membrane, siderophores are water soluble. The permeability and biological activity of siderophores is dictated by their three-dimensional structure and chirality, and the extent to which their shape fits specific membrane proteins.

Significant achievements have been recorded in the preparation of synthetic ionophores that selectively transport metal- or ammonium ions across membranes[7-12]. Remarkable progress has also been made with the preparation of siderophore analogs[4,13-14], although the requirements for obtaining biologically active molecules are much more stringent. For a binder to exhibit siderophoric properties it has to fulfill two requirements: (i) to effectively bind iron(III), and (ii) to fit membrane receptors and transport proteins whose structures are largely unknown.

We have adopted a biomimetic[15] scheme towards the design and synthesis of siderophore analogs[16-20] that helped us to gradually approach the properties of the natural counterparts both *in vitro* and *in vivo*. The biomimetic design relies on identifying the essential features of the natural compounds, and on reproducing these very features with the simplest possible synthetic molecules. We initiated our work by examining the structure of the natural siderophore Enterobactin[21] as a guiding model, and then reproduced these features with synthetic compounds so as to provide biomimetic analogs of both Enterobactin[16] and Ferrichrome[17-19] (see Figure 1).

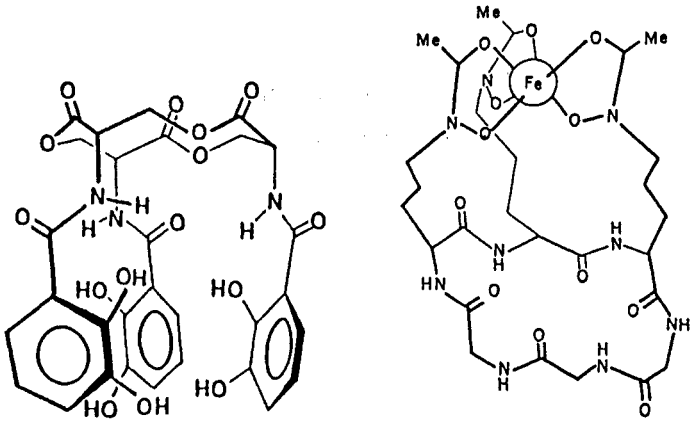


**Figure 1:** Enterobactin (left) and Ferrichrome (right).

We have so far synthesized analogs of Ferrichrome[17-19], that fully reproduce its iron(III) binding selectivity, efficiency, chiral preference and its biological activity as microbial iron(III) carrier. By comparing the activity of our siderophore analogs, much has been learned about the structure of the respective membrane components and their mode of recognition. Other siderophore analogs were prepared that mimicked the natural siderophore Enterobactin[16], approaching its selectivity, efficiency and chiral preference; their biological activity still awaits experimental study.

The common theme that threads through every stage of this work, and gave this article its title, is the contribution of weak, non-covalent interactions in dictating ion binding efficiency, conformational characteristics and biological activity. We shall restrict our discussion to H-bonds and van-der-Waals forces, and to a qualitative, rather than quantitative examination of the contribution of these interactions, except for isolated cases.

In the next section, our biomimetic modus operandi is presented and discussed. The subsequent sections contain a critical discussion of the various families of our biomimetic siderophore analogs, their synthesis, their physico-chemical properties and their biological performance. Finally we indicate possible applications of biomimetic chemistry beyond those discussed in detail here.

## 2. BIOMIMETIC DESIGN

The major characteristics of a natural ion-carrier is its binding site or cavity. The remaining part of the molecule is structured to support the binding site, and to be recognized by specific membrane components for transporting the complex into the cell. Natural ion-carriers achieved these features as a result of selection, and are produced by the biosynthetic machinery of the living cell.

Our biomimetic scheme draws from the evolutionary edge of the natural molecules and applies rational design to the maximum extent available, leaving the rest for trial and error. It is based on the following guide-lines:

Interactive experimental-theoretical strategy of examination[22]. The feasibility of a molecule to function as an ion carrier involves a finely tuned balance between the free energies of ion-complexation and of ion-hydration, that are both very large quantities. The fine tuning involves the conformational changes imposed on the ion-carrier by the formation of the complex. These conformational changes were studied both experimentally, by various spectroscopic methods, and theoretically, by the empirical force field method, (also named molecular mechanics)[22]. Theoretical calculations examined whether a designed molecule has a reasonable chance to bind the selected ion. Among many designed molecules, those that were predicted to be better ion-carriers were preferred for synthesis. Experiment determined the stoichiometry of binding as well as various conformational properties of the free and the complexed ion carrier. The calculated conformations then helped to interpret and correlate experimental results and put them into a coherent structural framework. Remaining discrepancies between theory and experiment guided us to re-evaluate both. Thus, experiment and theory were linked in a mutually supporting, interactive and iterative manner.

Symmetry. We tried to imitate natural ion carriers that possess inherent structural symmetry, or to synthesize symmetric analogs of non-symmetric structures. Symmetry is not an essential property, but contributed greatly to the economy of effort, both in the synthesis and in the interpretation of the observed properties of the product. Furthermore, while one might expect that membrane receptors of asymmetric natural ion-carriers would require that synthetic analogs would retain that asymmetry, this is not necessarily the case, as will be shown in the following sections.

Modular design. An ion carrier is a composite structure, and may be conceived as a combination of several components, or modules. Each module may be modified independently. All possible combinations of all modifications of the modules are *a priori* candidates for synthesis, but most of them were eliminated, or modified after synthesis and evaluation, using the above mentioned guide-lines plus some chemical common-sense. Once a certain combination of the modules proved to yield an efficient ion-carrier, systematic modifications of the appropriate modules yielded families of ion-carriers of gradually improved characteristics. Examples will be discussed in the subsequent sections.

## 3. RESULTS

### 3.1. Enterobactin and its H-bond network

The most potent iron(III) binder so far known is the siderophore Enterobactin (Figure 1, left)[4,5,23]. Enterobactin is a $C_3$-symmetric Triscatecholate composed of a trilactone ring as anchor and three pending side chains possessing ion binding sites that embed the guest ion in an octahedral cavity of a preferred $\Delta$-cis

configuration, dictated by the asymmetric centers of the trilactone ring. In the absence of asymmetric centers in the ligand, the two possible isomers, $\Delta$-cis and $\Lambda$-cis, are enantiomeric, energetically equivalent and equally populated. In the presence of chiral centers, the two configurations become diastereomeric and energetically different, such that either of one may be preferentially formed. Most of the natural siderophores possess chiral centers and form iron(III) complexes of either preferential $\Delta$-cis or $\Lambda$-cis configurations.[4,5,6,25]

We selected Enterobactin as a guiding model because of its exceptional potency which derives from its three dimensional structure. Comparison between Enterobactin and a large variety of synthetic analogs had earlier established the superiority of Enterobactin in exceeding the binding efficiency of related single-chain analogs by 10 orders of magnitude. When placing three catecholate residues on a Tris(aminomethyl)benzene as anchor, Raymond et al. obtained a $C_3$-symmetric Triscatecholate $C_6H_3\{CH_2NHCOC_6H_3(OH)_2\}_3$ (MECAM), which was a significantly more efficient binder than the single stranded analogs, but still inferior to Enterobactin by six orders of magnitude[4,20,23] Since the natural Enterobactin and the synthetic MECAM make use of the same binding sites, we concluded that the superiority of the natural siderophore derives from its structural features[16,20].

In an attempt to identify the structural origin of Enterobactin's iron(III) binding efficiency, we synthesized and examined its structural analog, the tribenzamide TBA[21], cyclo-$[OCH_2CH(NHCOC_6H_5)CO]_3$. TBA is the same as Enterobactin except for its missing hydroxyl groups. Due to the absence of the hydroxyl groups, TBA is unable to bind iron(III). On the other hand, TBA lends itself to a thorough spectroscopic examination which is not possible with the natural Enterobactin. The synthesis of TBA was accomplished by a template method we had earlier developed for the preparation of the trilactone ring skeleton[26], and for the total synthesis of Enterobactin[27].

Spectral examination of TBA, specifically IR- and NMR-spectroscopy, demonstrated the presence of intra-molecular H-bonds between the amide NH groups of the side chains and the lactonic oxa groups of the ring which direct the conformation of TBA towards a propeller-like arrangement[21]. CD-spectroscopy of TBA indicated exciton coupling between the benzoyl residues and helped to deduce preferential right-handed chiral sense for this molecule's propeller-like arrangement. Trisbenzamide thus adopts a conformation with the same handedness as that found for the Enterobactin-iron(III) complex[4].

Empirical Force Field calculations confirmed the conclusions drawn from experiment and linked the experimentally deduced conformational features of TBA with those of Enterobactin and its iron(III) complex (Figure 2)[21].

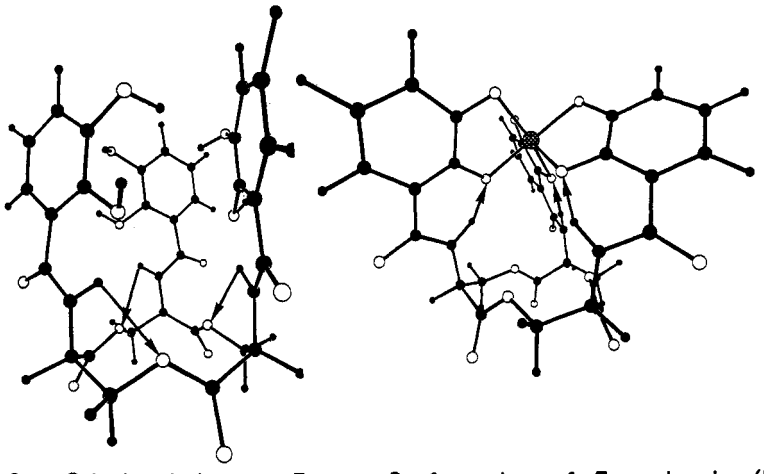

**Figure 2:** Calculated Lowest Energy Conformation of Enterobactin (left) and Enterobactin-iron(III) complex (right). Empty circles denote oxygen, H-bonds are indicated by arrows.

Comparison between the calculated lowest energy conformation of Enterobactin and of its iron(III) complex revealed striking similarities. The free ligand and its iron(III) complex are interrelated by H-bond networks; upon complexation the H-bonds pointing from the amide NH to the ring oxygens shift to the adjacent catecholate oxygens. This shift actually involves a radial movement of the H-bond from the ring anchor to the side chains, similar to that occurring in the windshield wipers of our cars. We therefore like to coin for this shift the term "wiper H-shift".

Since the presence of H-bond networks in the free ligand and the complex, and since their rearrangement when passing from the free to the complexed state appear to be the major differences between Enterobactin and the synthetic Triscatecholate MECAM, we attributed Enterobactin's exceptional iron(III) binding properties to these very features[20,21]. The H-bond network and "wiper-H-shift" was thought to favorably effect iron binding in two ways. In the free ligand the H-bonds shape the molecule towards a conformation which is predisposed for iron binding and thereby minimizes entropy loss upon binding. Upon binding, the rearranged H-bonds stabilize the complex formed and dictate its chiral sense. In an attempt to obtain biomimetic iron(III) binders that would simulate the favorable properties of the natural compound, we aimed at reproducing the H-bond networks observed in Enterobactin.

### 3.2. $C_3$-symmetric, H-bonded ion binders

Aiming at artificial iron(III) binders that would approach the properties of Enterobactin, we searched for molecules that (i) are strain-free when binding ferric ions, and that (ii) simulate Enterobactin by generating non-covalently defined ion binding cavities already prior to binding, and by undergoing the "wiper H-shift" upon binding.

Towards this goal, and for considerations of economy, we conserved Enterobactin's tripodal topology, but replaced the macrocyclic anchor by a readily available trifunctional anchor. In order to generate propeller-like conformations similar to that occurring in Enterobactin, we aimed to interlink the tripodal arms directly with each other through H-bonds, rather than orient them through H-bonds with the anchor.

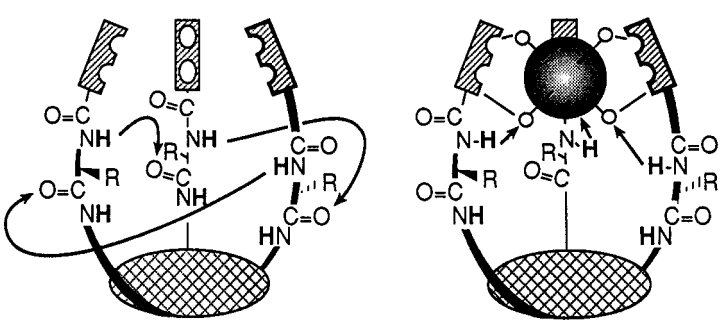

**Figure 3:**
**Artificial Ion Binders designed to undergo H-Bond Shifts upon binding.**

These ideas were realized by assembling ion binders in a modular fashion from a $C_3$-symmetric anchor through $C_3$-symmetric extensions with amino acid residues as structural elements, to terminal catecholates or hydroxamates as ion binding groups. In these binders the structural elements were deliberately separating the binding elements from the common anchor in order to enable independent modification of each till optimal performance is achieved.

A unique element in this design is the use of amino acids as structural elements. The amino acids fulfill three functions: (i) They form intramolecular H-bonds by virtue of their amide linkages and other non-covalent interactions by virtue of their side chains, (ii) they enable systematic modifications by varying the sidechains of the amino acid residues, and (iii) they impart chiral preference to the binders' complexes by virtue of their asymmetric centers. The latter feature is of paramount importance in view of the documented chiral discrimination of siderophore receptors and transport proteins[28,29].

### *3.2.1. $C_3$-symmetric triscatecholates as enterobactin analogs: enhanced binding efficiency by H-bond networks*

In line with the above considerations, two families of compounds were considered as chiral Enterobactin analogs: namely Type 1 and 2 Triscatecholates that are derived from the parent Trispeptides (Type 1 and 2) by extension with catecholate binding sites (Figure 4)[16]. In order to establish whether and to what extent these molecular skeletons adopt conformationally restricted arrangements, the parent Trispeptides were first examined.

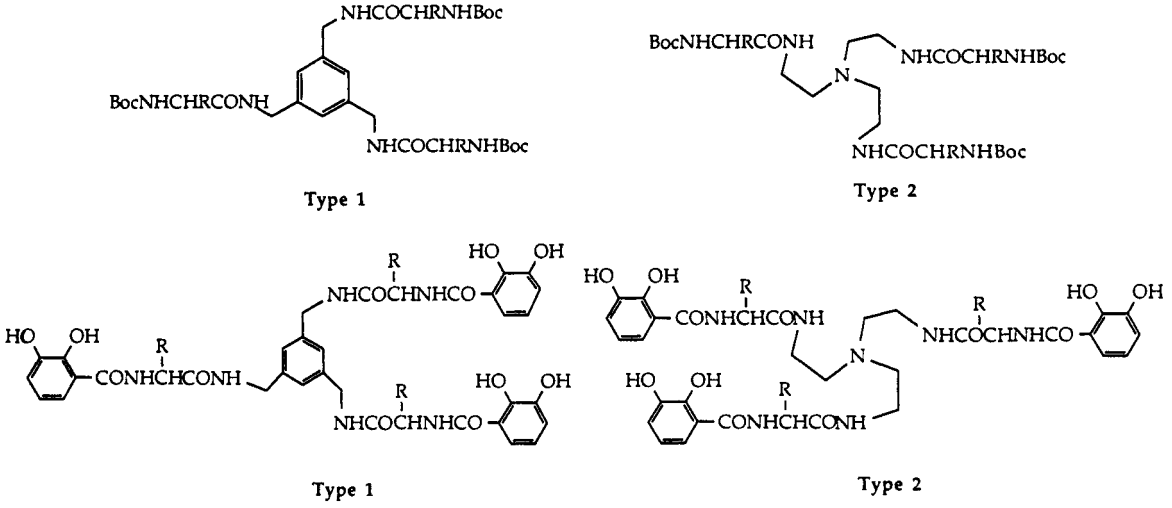


**Figure 4:** Type 1 and 2 Trispeptides (top) and Triscatecholates (bottom).

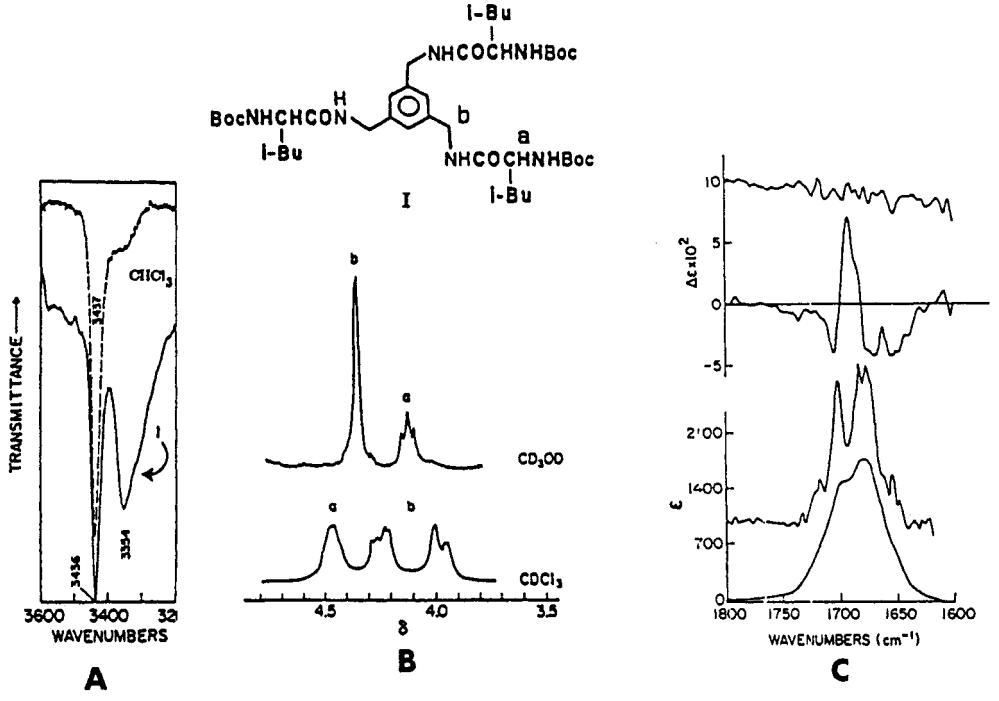


**Figure 5:** Partial IR-Spectrum (left), NMR-Spectra (middle) and VCD-Spectrum (right) of Type 1 Trispeptide. 5A: The solid line represents the IR-trace of the Trispeptide, the broken line that of its single strand analog. 5B: The upper trace shows the signals for the $\alpha$ -proton (a) and the diastereotopic protons $ArCH_2$- (b) in deuterated methanol, the lower one in deuterated chloroform. 5C: The traces from bottom to top show: the IR-absorption, the Fourier self-deconvolution of the IR-absorption, the Vibrational Circular Dichroism of the same absorption and the estimated instrumental noise.

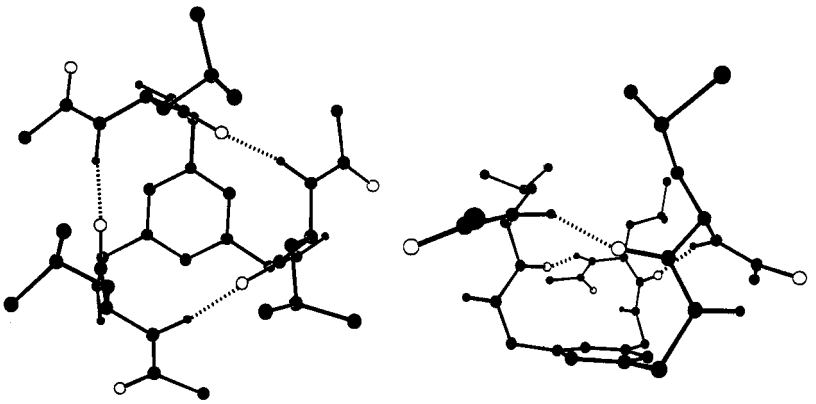

**Figure 6:** Calculated Lowest Energy Conformation of Type 1 Trispeptide (left, top view; right, side view). All hydrogens are omitted except for NH. Empty circles denote oxygen. H-bonds are denoted by dotted lines.

IR- and $^1$H-NMR spectroscopy of Type 1 leucyl Trispeptide (in comparison with the single chain analog $C_6H_5CH_2NHCOCHiBuNHBoc$) established the presence of inter-strand H-bonds that restrict the conformational freedom of the molecules' individual arms (Figures 5A and 5B)[30]. Vibrational Circular Dichroism (VCD) demonstrated that the inter-strand H-bonds have a preferred chiral sense such as to create a right-handed, propeller-like conformation (Figure 5C)[31].

Empirical Force Field calculations confirmed the conclusions drawn from experiments and resolved the equilibrium mixtures of conformations into their components[30]. Although the $C_3$-symmetric, right-handed propeller proved to be preferred (Figure 6), other non-symmetric conformations as well as the diastereomeric left-handed propeller are likely to be present at equilibrium.

All the experiments listed above were also performed on Type 2 leucyl Trispeptide (Table 1). Comparison between the two types showed a pronounced superiority of Type 2 derivatives in adopting conformationally restricted arrangements, and the advantage of hydrophobic amino acid residues. This was indicated by the higher proportion of bonded NH frequencies in the IR-spectrum, by the higher anisotropy ratio in the VCD-spectrum, and by the higher chemical shift difference of the diastereotopic protons in the NMR-spectrum of the Type 2 Trispeptide (Table 1).

**Table 1.** IR, VCD and $^1$H NMR Data of Representative Type 1 and Type 2 Trispeptides

| | IR[a] | VCD[b] | NMR[c] |
|---|---|---|---|
| | $NH_{bonded}/NH_{free}$ | $\nu$(CO–) $10^5\ \Delta\varepsilon/\varepsilon$ | $-CH_2NH-$ $\delta$ (ppm) |
| | (5·10$^{-4}$ M, $CDCl_3$) | (5·10$^{-4}$ M, $CHCl_3$) | (2.5·10$^{-3}$ M, $CDCl_3$) |
| *Type 1 Trispeptides* | | | |
| L-ala | 0.53 | 2.3 | 4.41(d); 4.17(d) $\Delta\delta$ = 0.24 |
| L-leu | 0.78 | 8.3 | 4.36(d); 4.02(d) $\Delta\delta$ = 0.34 |
| *Type 2 Trispeptides* | | | |
| L-leu | 5.0 | 20.8 | 3.47(d); 2.93(d) $\Delta\delta$ = 0.54 |

a) Intensity ratios for the absorptions of the bonded NH and free NH frequencies.
b) Anisotropy ratios $\Delta\varepsilon/\varepsilon$ for the amide carbonyl as measured by VCD (Vibrational Circular Dichroism).
c) Chemical shifts of the diastereotopic protons and chemical shift differences ( $\Delta\delta$) between the diastereotopic protons.

**Table 2.** IR and $^1$H NMR Data of Representative Type 1 and Type 2 Triscatecholates

| Compound | IR $\nu$(NH) $CDCl_3$ | NMR $\delta(CH_2NH)$ $CD_3OD$ |
|---|---|---|
| *Type 1 Triscatecholates* | | |
| (L-leu) | 3345; 3322 | 4.33 (s) |
| (L-ala) | | 4.35 (s) |
| *Type 2 Triscatecholates* | | |
| (L-leu) | 3257; 3277 | 3.38 (d); 3.21 (d) |
| (L-ala) | | 3.39 (d); 3.28 (d) |

Table 3. VIS- and CD- spectra and Relative Binding Efficiencies of Type 1 and Type 2 Triscatecholates

| Ligand | VIS[a] $\lambda_{max}$ ($\varepsilon$) | CD[a] $\lambda_{max}$ ($\varepsilon$) | | | Abs. Config. | Binding Ratio[b] | $K_L/K_M$[b] |
|---|---|---|---|---|---|---|---|
| *Type 1* | | | | | | | |
| (L-leu) | 502 (4650) | 432 (+4.2) | 502 (0.0) | 550 (–2.3) | Δ-cis | 7.3 | 50 |
| (L-ala) | 502 (4370) | 435 (+3.3) | 514 (0.0) | 560 (–1.0) | Δ-cis | -- | -- |
| (D-ala) | 502 (4460) | 435 (–3.3) | 514 (0.0) | 560 (+1.0) | Λ-cis | 6.7 | 45 |
| (N-Me-L-Leu) | 496 (4790) | 430 (–3.0) | 486 (0.0) | 540 (+2.1) | Λ-cis | 0.3 | 0.1 |
| *Type 2* | | | | | | | |
| (L-Leu) | 500 (5030) | 428 (+3.8) | 490 (0.0) | 540 (–2.9) | Δ-cis | >50 | >2500 |
| (L-ala) | 496 (5040) | 430 (+3.5) | 496 (0.0) | 548 (–1.6) | Δ-cis | 18 | 300 |
| Enterobactin | 494 (5330) | 420 (+4.0) | 435 (0.0) | 535 (–4.0) | Δ-cis | | $10^6$ |

[a]0.1 mM ferric complex in 10-15% MeOH in TRIS buffer 0.1 M pH 8.97. The $\lambda_{max}$ and $\lambda_{max}$ values are given in nm.
[b]The relative binding efficiency values are estimated from a CD monitored competition reaction between the chiral triscatecholate ligands and the nonchiral MECAM; $K_L/K_M$ is the ratio of the estimated binding efficiencies of the chiral ligand and MECAM.

Extension of both Trispeptide families with catecholates provided ion binders, whose conformations in the free state resembled those of the parent Trispeptides (Table 2). In chloroform solution, both Types of Triscatecholates were H-bonded, as indicated by their low-frequency NH-absorptions. Still, the lower NH-frequencies in Type 2 indicate stronger H-bonds in the latter. In methanol, Type 1 Triscatecholates adopted random conformations, while Type 2 Triscatecholates adopted restricted conformations, as shown by the appearance of identical or different signals for the respective diastereotopic protons. These features pronouncedly affected the molecules' ion binding properties: Type 2 Triscatecholates approached Enterobactin within less than three orders of magnitude, while the corresponding Type 1 Triscatecholates remained five orders of magnitude below Enterobactin (Table 3)[16].

That H-bonding in the complex is conducive to the complexes' stability and optical purity was further supported by comparing analogs of the same Type: replacement of the H-bond-donating amide NH by amide NMe in L-leu-Triscatecholate decreased the ligands' binding constant 500-fold and inverted its chiral preference to the non-natural Λ-cis configuration (Table 3). The preservation of the Δ-cis configuration in Enterobactin analogs may be crucial for obtaining biologically active compounds, since only the natural Δ-cis Enterobactin functions as microbial iron(III) carrier and growth promoter[28].

These data, taken together, demonstrate that preorganization of ion binders through H-bond networks and stabilization of the complexes by intra-molecular H-bonds provide better ligands in terms of binding efficiency and optical purity. The presence of H-bond networks was also found to enhance the binders' selectivity for iron(III) relative to other three-valent metal ions such as alumium(III), gallium(III) or indium(III)[16].

Of particular interest is the remarkably large range[4,20] of ion binding efficiencies observed for closely related catecholates and even Triscatecholates. This range exceeds by far that reported for other families of ion binders such as hydroxamates and Trishydroxamates[20]. The latter span a mere three order of magnitude, while catecholates span ten orders of magnitude. This observation might be attributed to the stringent steric demand in order to minimize the energy of the triply charged H-bonded catecholamide complex. Fulfillment of this demand imposes substantial conformational constraints on the polycyclic catecholate complexes, such that subtle structural changes might have pronounced consequences in terms of ion binding efficiency.

### *3.2.2. $C_3$-symmetric ferrichrome analogs: conformational consequences of H-bond networks and microbial activity*

The results obtained with the Triscatecholates[16] encouraged us to apply similar principles to the preparation of Ferrichrome analogs (Figure 1, right). We chose Ferrichrome analogs as target molecules because of both structural and biological considerations.

Structurally, Ferrichrome[25] shares with Enterobactin its tripodal topology. It however differs from Enterobactin by making use of hydroxamate groups as ion binding sites, by lacking $C_3$-symmetry, by adopting preferentially the $\Lambda$-cis configuration, and by the electroneutrality of its complex. The extent to which the principles deduced for Enterobactin and its synthetic analogs would be applicable to Ferrichrome analogs, was therefore thought to indicate their general applicability.

Biologically, Ferrichrome is of interest because of its broad range of activity. Although produced merely by fungi, it is taken up by a large variety of microorganisms that have developed Ferrichrome-sensitive iron(III) uptake systems.

Nature has thus provided us with a versatile playground to examine the structural subtleties of synthetic Ferrichrome analogs by examining their fit to microbial recognition sites. On the other hand, synthetic Ferrichrome analogs may probe the structural requirements of membrane components.

In order to obtain biomimetic Ferrichrome analogs we assembled $C_3$-symmetric Trishydroxamates from two families of Triscarboxylates (Figure 7)[17].

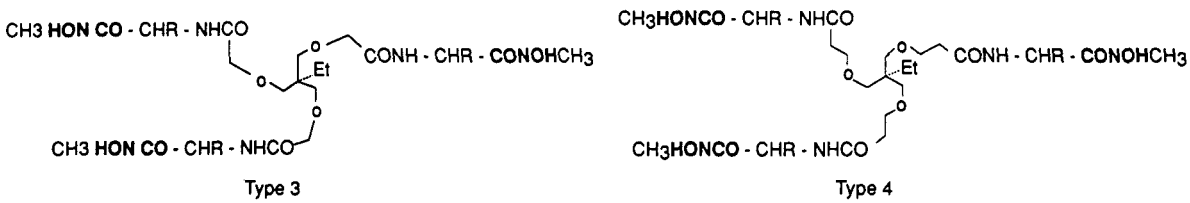


**Figure 7:** Type 3 and 4 Trishydroxamates.

Triscarboxylates, rather than Trisamines were selected as anchors, in order to enable attachment of the chiral amino acid bridges via their N-termini, rather than their C-termini and thereby invert the preferred chirality of the tripodal binders from a right-handed to a left-handed sense. The two homologous anchors, although differing only in one $CH_2$-group, provided two conformationally distinct families of complexes for *in vivo* testing.

In chloroform the two Types of Trishydroxamates showed low frequency NH and CO absorptions, and different chemical shifts for the diastereotopic protons (Table 4). In the more polar acetonitrile, the anisotropy of the diastereotopic protons collapsed to give single signals. These data indicate the presence of conformationally restricted arrangements that are stabilized by H-bonds. Comparison between these Trishydroxamates and selected reference compounds excluded the presence of mere intra-strand (Figure 8a) or inter-strand H-bonds (Figure 8b), but the formation of mutually supporting intra- and inter-strand H-bonds (Figure 8c)[17].

For the NMR studies of the complexes we replaced paramagnetic iron(III) by dimagnatic gallium(III). Both ions have similar ionic radii and have been shown to form hydroxamate complexes of similar crystal structures[32].

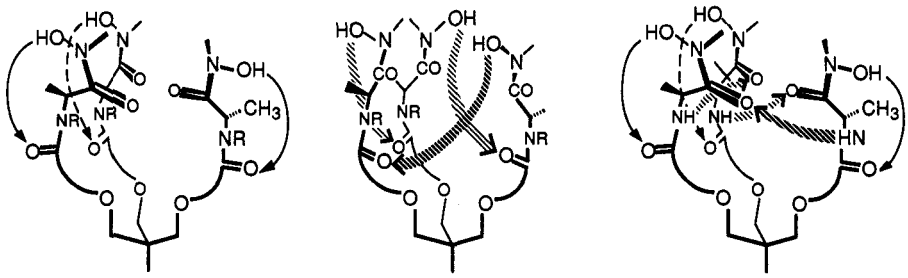

a, intra - strand b, inter - strand c, intra - and interstrand

**Figure 8:** Schematic Representation of H-Bonded Conformations of Type 3 and 4 Trishydroxamates.

**Table 4.** IR and $^1H$ NMR Data of Representative Type 3 (m=1) and Type 4 (m=2) Trishydroxamates

$$Et-C\left\{CH_2O(CH_2)_mCONHCHRCONOHCH_3\right\}_3$$

| Compound | | IR | | NMR | |
|---|---|---|---|---|---|
| | | ν(NH) | ν(C=O) | δ(C-$CH_2$-O·) | |
| m | R | ($10^{-2}$ M $CDCl_3$) | | ($10^{-2}$ M $CDCl_3$) | ($10^{-2}$ M $CD_3CN$) |
| 1 | H | | 1633[a] | | 3.63(s)[b] |
| 1 | $CH_3$ | 3397<br>3203 | 1642 | 3.50, ABq<br>(Δδ = 0.06) | 3.57(s) |
| 1 | iBu | 3408<br>3203<br>3155 | 1642 | 3.48, ABq<br>(Δδ = 0.07) | 3.49(s) |
| 2 | H | | 1641[a] | | 3.31(s)[b] |
| 2 | $CH_3$ | 3280 | 1632 | 3.17, ABq<br>(Δδ = 0.12) | 3.16(s) |
| 2 | iBu | 3284 | 1630 | 3.15, ABq<br>(Δδ = 0.08) | 3.16(s) |

a) in $10^{-2}$ M $CD_3CN$ b) in $10^{-2}$ M $CD_3OD$

NMR-spectroscopy of Type 3 and 4 Trishydroxamate gallium(III) complexes showed pronounced differences between the two Types and between their various derivatives (Table 5). While the diastereotopic protons of Type 1 glycyl derivative (R = H) gave rise to an unresolved NMR-pattern, those of Type 2 glycyl derivative (R = H) gave a single signal. When replacing glycyl (R = H) by either alanyl (R = $CH_3$) or leucyl (R = iBu), distinct sets of signals were observed for the diastereotopic protons of all gallium(III) complexes. These results indicate the formation of intricate mixtures of complexes from Type 1 glycyl derivative (R = H), but well defined complexes from all other Trishydroxamates, including the glycyl derivative (R = H) of Type 2. The presence of side chains appears thus essential in Type 1, but not in Type 2, to attain defined complexes of 1:1 stoichiometry, either by preventing the formation of oligomeric complexes, or by stabilizing monomeric complexes.

Table 5. $^1$H NMR Data of Galium(III) Trishydroxamates, IR and UV/CD Data of Iron(III) Trishydroxamates

(Type 3, m=1; Type 4, m=2)

$$Et-C\left\{CH_2O(CH_2)_mCONHCHRCONOHCH_3\right\}_3$$

| | m = 1 | | | m = 2 | | |
|---|---|---|---|---|---|---|
| R | NMR[a] δ(C-(-$CH_2$-O)) ($10^{-2}$ M $CD_3CN$) | IR[b] ν(NH) ν(C=O) ($10^{-2}$M $CDCl_3$) | CD[c] $\lambda_{ext}$ (Δε) (aq.MeOH) | NMR[a] δ(C-(-$CH_2$-O)) ($10^{-2}$ M $CD_3CN$) | IR[b] ν(NH) ν(C=O) ($10^{-2}$M $CDCl_3$) | CD[c] $\lambda_{ext}$ (Δε) (aq.MeOH) |
| H | multiple signals[d] | | | 3.65(s)[d] | | |
| $CH_3$ | 3.68, ABq (Δδ = 0.30) | | 374,420,452 (-6.0, 0.0, +2.7) | 3.70, ABq; 3.48, ABq (Δδ = 0.49) (Δδ = 0.19) | | 365,420,450 (-7.5, 0.0, +2.5) |
| iBu | 3.65, ABq (Δδ = 0.20) | 3410; 1675; 1600 | 372,420,452 (-6.7, 0.0, +3.0) | 3.81, ABq[e] (Δδ = 0.50) | 3346; 1664; 1601 | 365,415,450 (-6.8, 0.0, +3.43) |

a) The NMR pattern of the diasteretopic protons provide a measure for the isomeric purity of the complexes

b) The IR-spectra indicate the presence (or absence) of bonded NH and/or CO.

c) The absolute signs of the cotton effects in the CD spectra indicate preferred Λ-cis configuration.

d) $10^{-2}$ M $CD_3OD$.

e) $10^{-2}$ M $CDCl_3$.

The IR-spectra of the isolated iron(III) complexes showed the presence of iron(III) bound hydroxamate (around 1600 $cm^{-1}$) and free carbonyl amide (around 1670 $cm^{-1}$) in both Types of Trishydroxamates (Table 5). The two Types of Trishydroxamates differed in the NH-frequencies, showing free NH in Type 1, but bound NH in Type 2. These observations suggest that the amides are oriented tangentially to the complexes' cross section in Type 3, but oriented radially with the amide NH pointing into the molecules' interior in Type 4, forming H-bonds to the ether-oxygens and iron-oxygens (Figure 9). Independent of their detailed conformations, both Types of chiral iron(III) complexes showed similar CD-spectra, indicating preferential *Λ*-cis configuration, as in Ferrichrome (Table 5).

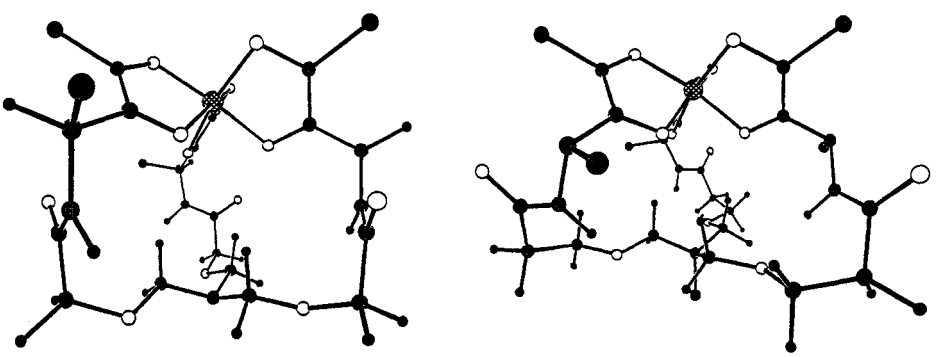

**Figure 9:** Calculated Lowest Energy Conformations of Type 3 (left) and Type 4 (right) Trishydroxamate iron(III) Complexes. The hydrogens of the methyl groups are omitted. Empty circles denote oxygens.

EFF calculations (Figure 9), and later also 2D-NMR- spectroscopy confirmed the above conclusions and emphasized the pronounced conformational differences between the two Types of Trishydroxamates, as deriving from the presence (or absence) of stabilizing H-bonds.

The conformational details of Type 3 and 4 Trishydroxamates determined also these compounds' microbial activity. When examined on mutants of *Pseudomonas putida*, representatives of Type 4 Trishydroxamates proved active[19], while none of the Type 3 Trishydroxamates showed any activity. For a siderophore or a siderophore analog to act as microbial iron(III) carrier, it has to transverse the microbial membranes by binding to the respective receptors of the outer membrane and the transport proteins of the cytoplasmic membrane. Most remarkably, Type 4 Trishydroxamate derived from glycine (R = H, Figure 10) fully reproduced the action of Ferrichrome by promoting microbial iron(III) uptake and growth with almost the same efficiency. Type 4 Trishydroxamate derived from L-alanine (R = Me, Figure 10) inhibited Ferrichrome mediated iron(III) uptake, while the enantiomer derived from D-alanine had no effect. These results suggest that the glycine derivative of Type 4 is recognized by both the microbial membrane receptor and transport system, while the L-alanine derivative of Type 4 merely binds to the membrane receptor such as to inhibit the action of Ferrichrome. When examined on *Arthrobacter flavescens*, the L-alanine derivative of Type 4 proved not to act as inhibitor, but as substitute of Ferrichrome with equal efficiency[18].

The latter findings have several implications. Firstly, they demonstrate, that it is indeed possible to simulate with all-synthetic iron(III) binders the performance of natural siderophores *in vivo*. Secondly, they illustrate the usefulness of synthetic binders as structural probes of microbial receptors and transport proteins. Thirdly, they demonstrate that siderophore mediated iron(III) uptake systems differ in their structural characteristics from species to species. And last but not least, these findings seem to pave the road towards species-specific iron(III) carriers that function either as species-specific growth promoters, or growth inhibitors.

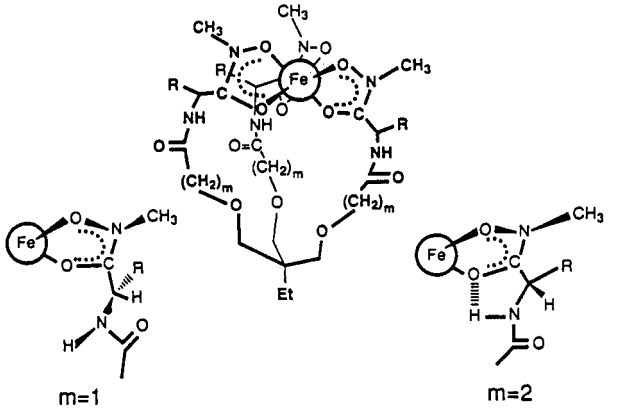


**Figure 10:** Structural Characteristics and Microbial Activity of Type 3 (m=1) and Type 4 (m=4) Trishydroxamates in *Pseudomonas putida*.

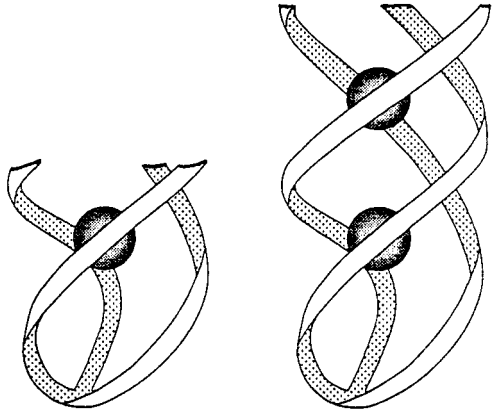

**Figure 11:** Schematic Representation of Triple-Stranded Complexes (left: mononuclear; right: dinuclear).

### 3.3. Triple-stranded polytopic ion binders

The tripodal topology is inherently fit for extension along the molecules' main axis to provide ditopic and polytopic ion binders. Dinuclear and polynuclear complexes derived from ditopic and polytopic binders (Figure 11) are versatile models for the study of metal-metal interactions and of ion transport phenomena as occurring in channel formers[33].

Towards this goal, a monotopic Trishydroxamate based on Type 2 Trispeptide (Figure 12, left) was extended via an intermittent amide group (Figure 12, middle) or intermittent ester group (Figure 12, right) to form an additional hydroxamate ion-binding cavity[34].

The VIS- and CD-spectra of the ditopic binders possessing intermittent amide or ester groups provided information on the effect of possible H-bonds on the complexes' structures[34]. They showed that the mononuclear complex preferentially adopted the left-handed, *Λ*-cis configuration, while the dinuclear complex with amide groups adopted a helical arrangement with the opposite, *Δ*-cis configuration around each metal center. This inversion of configuration was attributed to the formation of an extended H-bond network which affected the relative stability of the diastereomeric complexes. The reversal of the absolute configuration to the left-handed one in the dinuclear complex possessing intermittent ester groups supported this conclusion.

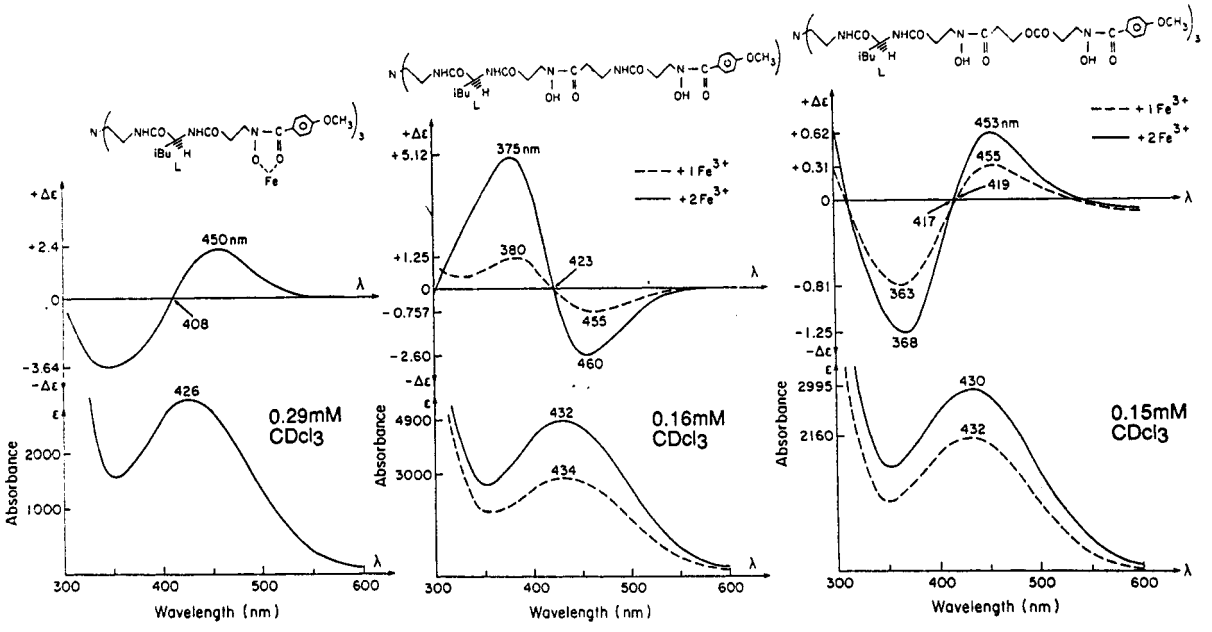


**Figure 12:** VIS- and CD- Spectra of Triple-Stranded Helical Iron(III) Complexes.

## 4. CONCLUSIONS

We have introduced novel families of hexadentate ion binders with superior properties in terms of binding efficacy and selectivity that reproduce the essential structural features of naturally occurring ion binders, specifically microbial siderophores. In this endeavor we followed an interactive-experimental-theoretical approach and adopted a modular strategy of design and synthesis, by linking three bidentate binding groups via amino-acid residues to $C_3$-symmetric anchors. The threefold symmetry inherently suited octahedral ion binding cavities. Thus some of our $C_3$-symmetric analogs of the asymmetric Ferrichrome fully reproduced its biological function. Moreover, the presence of a symmetry element greatly facilitated synthesis, theoretical treatment and interpretation of the ligands' observed properties. The most pertinent feature of these ligands and their complexes is the presence of non-covalent, intramolecular bonds. These non-covalent interactions restrict the conformations of the free ligands towards arrangements prone to ion binding, minimize entropy loss upon binding and stabilize the complexes once formed.

Since synthetic iron(III) carriers possess various biological activities, they provide superb structural probes of biological receptor sites. The advantage of synthetic carriers for biological applications resides in their versatility. In contrast to the natural siderophores, biomimetic analogs may be tuned to either act as growth promoters, or as growth inhibitors, and may even be tuned to have opposite activity towards different organisms. Moreover, the option to add fluorescent or radioactive labels at exogneous positions that do not interfere with receptor recognition opens new possibilities.

In more general terms, the synthesis of ion binding molecules may be regarded as a modest beginning towards the synthesis of task-oriented molecules. Recognition of a specific metal ion can be regarded as the most primitive case of molecular recognition. When coupled with elements for mass-transport and electron-transport, or with elements for signalling, such systems are believed to provide technologically useful devices by reproducing basic biological functions outside the living cell. Such systems could either be generated by introducing multiple functions into single molecular entities, or by joining molecules with complementary functions into molecular assemblies. Possibilities that are currently being explored by us and other groups are the creation of molecular sensors, molecular regulators or light harvesting systems.

**Acknowledgement** The authors thank their co-workers who are quoted in the references for their enthusiastic collaboration through the many stages of this work. Financial support from the US-Israel Binational Science Foundation, the Minerva Foundation and the Israel Academy for Sciences and Humanities is gratefully acknowledged. A.S. is holder of the Siegfried and Irma Ullmann Professorial Chair.

## REFERENCES

(1) Ovchinnikov, Yu.A. and Ivanov, V.T., *Tetrahedron*, 1975, *31*, 2177.
(2) Burgermeister, W., and Winkler Oswatitsch,R. *Topics in Current Chemistry*, 1977, *69*, 93.
(3) Neilands, J.B. *Structure and Bonding* 1984, *58*, 1.
(4) Raymond, K.N.; Mueller, G.; Matzanke, B.F. *Top. Current Chem.* 1984, *123*, 49, and references therein.
(5) Hider, R.C. *Structure and Bonding* 1984, *58*, 25.
(6) Matzanke, B.F.; Muller-Matzanke, G.; Raymond, K.N. *Iron Carriers and Iron Proteins* Loehr, T.M. (Ed.), VCH Publishers, NY, 1989, pp. 1.
(7) Pedersen, C.J. *Angew. Chem. Int. Ed. Engl.* 1988, *27*, 1021.
(8) Cram, D.J. *Angew. Chem. Int. Ed. Engl.* 1988, *27*, 1009.
(9) Cram, D.J. *Angew. Chem. Int. Ed. Engl.* 1986, *25*, 1039.
(10) Lehn, J.M. *Angew. Chem. Int. Ed. Engl.* 1988, *27*, 89.
(11) Weber, E.; Voegtle, F. *Host Guest Complexes Chemistry - Macrocycles*, Voegtle, F., Weber, E. (Eds.), Springer-Verlag, Berlin, 1985, pp. 1.
(12) Hilgenfeld, R.; Saenger, W. in *Host Guest Complexes Chemistry - Macrocycles*, Voegtle, F., Weber, E. (Eds.), Springer-Verlag, Berlin, 1985, pp. 43.
(13) Harris, W.R.; Carrano, C.J.; Cooper, S.R.; Sofen, S.R.; Avdeef, A.E.; McArdle, J.V.; Raymond, K.N. *J. Am. Chem. Soc.* 1979, *101*, 6097; Harris, W.R.; Raymond, K.N. *J. Am. Chem. Soc.* 1979, *101*, 6534; F.L., Weitl; Raymond, K.N. *J. Am. Chem. Soc.* 1979, *101*, 2728.
(14) Lee, B.H.; Miller, M.J.; Prody, C.A.; Neilands, J.B. J. Med. Chem., 1985, *28*, 317. Mitchell, M.S.; Walker, D.L.; Whelan, D.L.; Bosnich, B. Inorg. Chem., 1987, *26*, 396. Akiyama, M.; Katoh, A.; Muto, T. J. Org. Chem., 1988, *53*, 6089. Ng, Y.C.; Rodgers, S.J.; Raymond, K.N. Inorg. Chem., 1989, *28*, 2062.
(15) Breslow, R. *Acc. Chem. Res.*, 1980, *13*, 170.

(16) Tor, Y.; Libman, J.; Shanzer, A.; Lifson, S. *J. Am. Chem. Soc.* 1987, *109*, 6517. Tor, Y.; Libman, J.; Shanzer, A.; Felder, C.E.; Lifson, S. J. Am. Chem. Soc., 1992, in press.
(17) Tor, Y.; Libman, J.; Shanzer, A. J. Am. Chem. Soc., 1987, *109*, 6518. Dayan, I.; Libman, J.; Agi, Y.; Shanzer, A., submitted for publication.
(18) Shanzer, A.; Libman, J.; Lazar, R.; Tor, Y.; Emery, T. Biochem. Biophys. Res. Commun., 1988, *157*, 389.
(19) Jurkevitch, E.; Hadar, Y.; Chen, Y.; Libman, J.; Shanzer, A. 1992, J. Bacteriol., *174*, 78.
(20) Shanzer, A.; Libman, J. "*CRC-Handbook of Microbial Iron Chelates*", (G. Winkelmann, Edit.) CRC Press, Inc., 309, 1991.
(21) Shanzer, A.; Libman, J.; Lifson, S.; Felder, C.E. *J. Am. Chem. Soc.* 1986, *108*, 7609.
(22) For a description and of the EFF method and its early applications to ion carriers see: Lifson, S.; Felder, C.E.; Shanzer, A.; Libman, J. *Progress in Macrocyclic Chemistry*, Vol. 3, Izatt R.M. and Christensen J.J., Eds., John Wiley & Sons, N.Y. 1987, pp. 241.
(23) The latest binding constant for enterobactin was reported to be $\log K_f = +49$[24], which is three orders of magnitude lower than earlier reported.[4] This difference is due to differences in the pK values of the free ligand, rather than to differences in the affinity of the deprotonated catecholate to $Fe^{3+}$. It is therefore concluded, that the binding constant for MECAM is also three orders of magnitude lower than originally reported[4], namely $\log K_f = +43$ rather than +46.
(24) Loomis, L.D.; Raymond, K.N., *Inorg. Chem.* 1991, *30*, 906
(25) Burnham, B.F.; Neilands, J.B. J. Biol. Chem., 1960, *236*, 554. Emery, T. Biochemistry, 1971, *10*, 1483. Van der Helm, D.; Baker, J.R.; Eng-Wilmot, D.L.; Hossain, M.B.; Loghry, R.A. J. Am. Chem. Soc., 1980, *102*, 4224.
(26) Shanzer, A.; Libman, J.; Frolow, F. *J. Am. Chem. Soc.*, 1981, *103*, 7339.
(27) Shanzer, A.; Libman, J. *J. Chem. Soc., J. Chem. Soc. Chem. Commun.*, 1983 846.
(28) Neilands, J.B.; Erickson, T.J.; Rastetter, W.H. *J. Biol. Chem.* 1981, *256*, 3831.
(29) "Iron Transport in Microbes, Plants and Animals", Winkelmann, G., van der Helm, D. and Neilands, J.B., (Edit.), VCH Verlagsgesellschaft mbH, D-6940 Weinheim, Germany (1987). Winkelmann, G. and Braun, V., FEMS Microbiol Letters , 1981, *11*, 237.
(30) Tor, Y.; Libman, J.; Shanzer, A.; Felder, C.E.; Lifson, S. *J. Chem. Soc. Chem. Comm.* 1987, 749. Tor, Y.; Libman, J; Shanzer, A.; Felder, C.E.; Lifson, S. *J. Am. Chem. Soc.*, 1992, in press.
(31) Paterlini, M.G.; Freedman, T.B.; Nafie, L.A.; Tor, Y.; Shanzer, A. *Biopolymers*, 1991, in press.
(32) Bargias, B.A.; Barclay, S.J., Raymond, K.N., *J. Coord. Chem.* 1986, 109. *15*,
(33) Urry, D.W. *Topics in Current Chemistry*, 1985, *128*, 175. Eisenman, G.; Dani, J.A. *Ann. Rev. Biophys. Biophys.* 1987, *16*, 205; Changeux, J.P.; Giraudat, J.; Dennis, M. *Trends Pharmacol. Sci.*, 1987 *8* (12), 459.
(34) Libman, J.; Tor, Y.; Shanzer, A. *J. Amer. Chem. Soc.*, 1987, *109*, 5880.